Spatial Distribution of Inhibitory Interneurons Expressing Calcium Binding Proteins in Turtle Visual Cortex

Timothy Sweeney and Philip Ulinski*

Committee on Computational Neuroscience, The University of Chicago

Abstract

Visual stimuli evoke waves of electrical activity that propagate across the visual cortex of freshwater turtles and code information about stimuli in visual space. The origination, speed and duration of these waves are controlled, in part, by three populations of inhibitory interneurons. Describing the spatial distribution of these cells is a necessary step in understanding cortical mechanisms. This study uses calcium binding proteins as markers for populations of inhibitory neurons in order to characterize their spatial distributions in the cortex.

Keywords: Cortical waves, Feedback inhibition, Feedforward inhibition

1. Introduction

Visual stimuli elicit propagating waves of activity in the visual cortex of freshwater turtles. These waves can be visualized using multielectrode arrays [6, 7] or voltage sensitive dyes [8] and are believed to code information about the positions of stimuli in visual space [4]. Recent simulation studies from our laboratory suggest that inhibitory interneurons play a major role in controlling the generation, speed and duration of cortical waves [9]. Turtle visual cortex contains at least three populations of inhibitory interneurons which differ in their morphology, physiology and functional roles [1]. Subpial cells have their somata positioned in the outer half of the external layer of the cortex (layer 1). Their dendrites are embedded in the fascicle of geniculate afferents that crosses visual cortex from lateral to medial. They show a regular spiking (RS) firing pattern that is characterized by a distinct spike rate adaptation. Subpial cells are implicated in controlling the origination and speed of cortical waves. Stellate cells have somata positioned in the inner half of layer 1 and dendrites that ascend into the geniculate afferents while other dendrites descend into layer 2. Both sets of dendrites are positioned to receive excitatory inputs from the collaterals of pyramidal cells. They show a fast spiking (FS) firing pattern that demonstrates little spike rate adaptation. Stellate cells play a minor role in controlling wave speed but a major role in controlling wave duration. Horizontal cells have their somata and dendrites positioned in layer 3 and are dominated by the collaterals of pyramidal cells. Like stellate cells, they have an FS firing pattern. They are involved principally in regulating wave duration.

A striking feature of turtle visual cortex is that there is a distinct spatial inhomogenity in the distribution of cells within the three layers of the cortex. Pyramidal cells are the dominant cell population in the intermediate, layer 2 of the cortex. Reasonable estimates of the spatial distribution of pyramidal cells can, thus, be constructed by plotting the distribution of layer 2 neurons in Nissl preparations. However, the external layer 1 contains both subpial and stellate cells, which are not easily disinguished in Nissl preparations. However, it is now well established

* Corresponding author
E-mail address: pulinski@uchicago.edu

that morphologically and physiologically distinct populations of inhibitory interneurons express different molecular markers in mammalian cortex (e.g [3]). Calcium binding proteins have proven particularly useful in labelling populations of inhibitory interneurons. Large basket cells, for example, typically express the calcium binding protein, parvalbumin [5]. In this study, we used immunohistochemical methods to detect parvalabumin immunopositive neurons and then chart their laminar and areal distributions.

2. Methods

Turtles were anesthetized and perfused with 0.12 M phosphate buffer followed by 4% paraformaldehyde in phosphate buffer. Brains were embedded in gelatin and left in 4% paraformaldehyde with 30% sucrose for two days. Brains were sectioned on a cryostat at –26° C into 30 μm sections. Free-floating sections were placed in 0.2% Triton X-100 for 30 minutes, and then exposed to Sigma anti-parvalbumin antiserum overnight. Sections were stained using a Vector Laboratories ABC kit, and developed with diaminobenzidine for 15 minutes. Sections were then mounted and cleared. Detailed *camera lucida* drawings of layer 1 and layer 3 cells were made at 16X magnification. Drawings were scanned and analyzed using the NIH Image software package. The distance of each cell from the ependymal surface was measured and plotted as a function of the distance from the junction of the cortex from the anterior dorsal ventricular ridge.

3. Results

Parvalbumin immunopositive neurons were found in all three layers of the cortex in several well-stained brains. There was heavy labeling in layer 2, suggesting that majority of pyramidal cells express parvalbumin. Labeled neurons were also seen in layers 1 and 3. Layer 1 immunopositive neurons had oval or spherical somata. Layer 3 immunopositive neurons had fusiform somata with the long axes parallel to the ependymal surface. Figure 1 shows the distance of each parvalbumin positive soma in layers 1 and 3 in a single well-labeled brain plotted as a function of it distance from the junction of the cortex with the anterior ventricular ridge. The spatial distribution of parvalbumin immunopositive neurons in this brain was consistent with distributions in other brains. Neurons positioned near the lateral edge of the cortex had distances near zero while those positioned more medially in the cortex had larger positive values. Labeled neurons with somata in layer 1 are localized in the inner half of layer 1. The distance of labeled neurons from the ependyma decreases systematically along the lateral-medial axis of the cortex following the decrease in the distance of layer 2 from ependymal surface. The density of labled neurons is approximately constant along the lateral-medial axis of the cortex. Labeled neurons with somata in layer 3 are spread evenly along the ependymal-pial axis of the layer. However, their density decreases along the lateral-medial axis of the cortex, reflecting the decrease in the thickness of the layer along this axis of the cortex.

4. Discussion

The expression of parvalbumin by inhibitory interneurons has been emphasized in the literature, but most studies report that a percentage of pyramidal cells also express parvalbumin immunoreactivity. Layer 2 cells in turtle visual cortex express strong parvalbumin immunoreactvity, suggesting that a larger percentage of turtle pyramidal cells express parvalbumin than have been reported in mammalian cortex. The morphology and localization of parvalbumin immunopositive somata in the lower half of layer 1 correspond to the morphology and spatial distribution of stellate cells in studies in which cells are characterized via intracellular recording methods and then filled with *Neurobiotin*. This suggests that parvalbumin immunopositive neurons include stellate cells. This finding is consistent with the tendency reported in the literature on

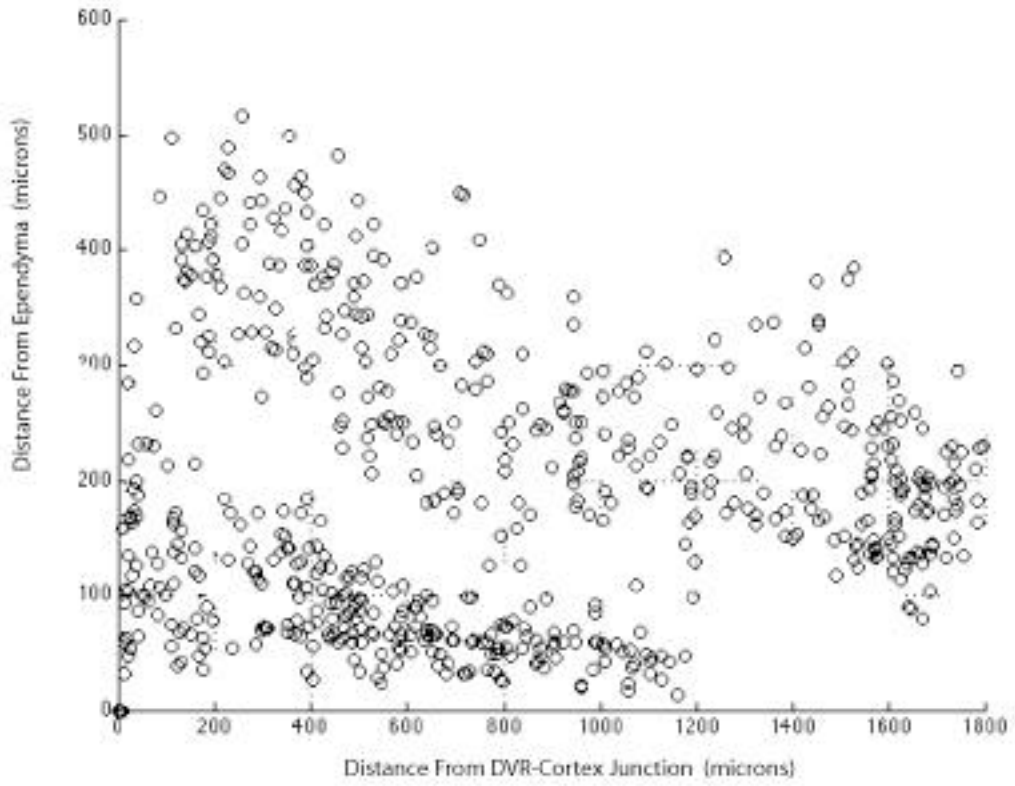

Figure 1. Spatial distribution of parvalbumin immunopositive neurons in turtle visual cortex. The distance of each parvalbumin immunopositive neurons from the ependymal surface of the cortex is plotted as a function of the junction of the cortex with the anterior dorsal ventricular ridge (distance value of zero) in a well-stained brain.

mammalian cortex for neurons which express parvalbumin to show an FS firing pattern. The pattern of parvalbumin immunoreactivity suggests that stellate cells are evenly distributed along the lateral-medial and rostral-caudal axes of the cortex. There was relatively little parvalbumin immunoreactivity in the outer half of layer 1. This suggests that few, if any, subpial cells express parvalbumin. The morphology of the parvalbumin immunopositive cells in layer 3 suggest that the majority of horizontal cells express parvalbumin. This finding is also consistent with a relationship between parvalbumin expression and a FS firing pattern. The spatial distribution of layer 3 immunoreactivity suggests that horizontal cells have a greater density in the lateral half of layer 3 than they do in the medial half.

Acknowledgement

This work was supported by a grant from the Collaborative Research in Neuroscience program from the National Science Foundation.

References

[1] Colombe, J. B., J. Sylvester, J. Block and P. S. Ulinski (2004) Subpial and stellate cells: Two populations of interneurons in turtle visual cortex. J. Comp. Neurol., in press.

[2] Connors, B. W. and A. R. Kriegstein (1986) Cellular physiology of the turtle visual cortex: distinctive properties of pyramidal and stellate neurons. J. Neurosci. 6: 164 - 177.

[3] Kawaguchi, Y. and Y. Kubota (1993) Correlation of physiological subgroupings of nonpyramidal cells with parvalbumin- and calbindin$_{D28k}$-immunoreactive neurons in layer V of rat frontal cortex. J. Neurophysiol. 70: 387 – 396.

[4] Nenadic, Z., B. K. Ghosh and P. S. Ulinski (2002) Modelling and estimation problems in the turtle visual cortex. IEEE Trans. Biomed. Eng. 49: 753 - 762.

[5] Palwelzik, H, D. I. Hughes and A. M. Thomson (2002) Physiological and morphological diversity of immunocythochemically defined parvalbumin - and cholecystokinin-positive interneurones in CA1 of the adult rat hippocampus. J. Comp. Neurol. 443: 346 - 367.

[6] Prechtl, J. C., L. B. Cohen, P. P. Mitra, B. Pesaran and d. Kleinfeld (1997) Visual stimuli induce waves of electrical activity in turtle cortex. Proc. Nat. Acad. Sci. 97: 877 – 882.

[7] Prechtl, J. C., T. H. Bullock and d. Kleinfeld (2000) Direct evidence for local oscillatory current sources and intracortical phase gradients in turtle visual cortex. Proc. Natl. Acad. Sci. 97: 977 – 882.

[8] Senseman, D. M. (1999) Spatiotemporal structure of depolarization spread in cortical pyramidal cell populations evoked by diffuse retinal light flashes. Vis. Neurosci. 16: 65 - 79.

[9] Ulinski, P. S., W. Wang and B. Ghosh (2003) Generation and control of propagating waves in visual cortex. Proc. 42nd IEEE Conference on Decision and Control, pp. 6429 – 6434.